https://doi.org/10.5194/egusphere-2025-3149
Preprint. Discussion started: 25 July 2025

Drivers of Phytoplankton Bloom Interannual Variability in the Amundsen and Pine Island Polynyas

Guillaume Liniger[1,2,3*], Delphine Lannuzel[1,4,5], Sébastien Moreau[6,7], Michael S. Dinniman[8], Peter G. Strutton[1,2,4]

[1] Institute for Marine and Antarctic Studies, University of Tasmania, Hobart, Australia

[2] Australian Research Council Centre of Excellence for Climate Extremes, University of Tasmania, Hobart, Australia

[3] Monterey Bay Aquarium Research Institute, Moss Landing, CA, USA

[4] Australian Centre for Excellence in Antarctic Science, University of Tasmania, Hobart, Australia

[5] Australian Antarctic Program Partnership, University of Tasmania, Hobart, Australia

[6] Norwegian Polar Institute, Tromsø, Norway

[7] iC3: Centre for ice, Cryosphere, Carbon and Climate, Department of Geosciences, UiT The Arctic University of Norway, 9037 Tromsø, Norway

[8] Center for Coastal Physical Oceanography, Old Dominion University, Norfolk, VA, USA

* Corresponding Author: Guillaume Liniger (liniger@mbari.org)

Abstract

The Amundsen Sea Embayment (ASE) experiences both the highest ice shelf melt rates and the highest biological productivity in West Antarctica. Using 19 years of satellite data and modelling output, we investigated the long-term influence of environmental factors on the phytoplankton bloom in the Amundsen sea (ASP) and Pine Island polynyas (PIP). We tested the prevailing hypothesis that changes in ice shelf melt rate could drive interannual variability in the polynyas' surface chlorophyll-*a* (chl*a*) and Net Primary Productivity (NPP). We found that the interannual variability and long-term change in glacial meltwater may play an important role in chl*a* variance

https://doi.org/10.5194/egusphere-2025-3149
Preprint. Discussion started: 25 July 2025

in the ASP, but not for NPP. Glacial meltwater does not explain the variability in both chl*a* and NPP in the PIP, where light and temperature are the main drivers. We attribute this to potentially greater amount of iron-enriched meltwater brought to the surface by the meltwater pump downstream of the PIP, and the coastal ocean circulation accumulating and transporting iron towards the ASP.

Short Summary

Our study investigates the links between the phytoplankton bloom and environmental parameters in the Amundsen polynyas (areas of open water within sea ice). Between 1998 and 2017, we find that changes in melting ice shelves may have different impacts on biological productivity between the Pine Island (PIP) and Amundsen Sea (ASP) polynyas. While ice shelf melting seems to play an important role for phytoplankton growth in the ASP, light and warmer waters appear to be more important in the PIP.

1. Introduction

Coastal polynyas are open ocean areas formed by strong katabatic winds pushing sea ice offshore (Morales Maqueda, 2004). They are the most biologically productive areas in the Southern Ocean (SO) relative to their size (Arrigo et al., 1998). This high biological productivity contrasts sharply with the rest of the SO, where low iron and light availability generally co-limit phytoplankton growth (Boyd et al., 2007). In West Antarctica, the Amundsen Sea Embayment (ASE) hosts two of the most productive Antarctic polynyas: The Pine Island Polynya (PIP) and Amundsen Sea Polynya (ASP; Arrigo & van Dijken, 2003). The ASE is also the Antarctic region experiencing the highest mass loss from the Antarctic ice sheet. It has been undergoing increased calving, melting, thinning and retreat over the past three decades (Paolo et al., 2015; Rignot et al., 2013; Rignot et al., 2019; Shepherd et al., 2018). In the ASE, this ice loss is mainly through enhanced basal melting of the ice shelves, which is attributed to an increase in wind-driven Circumpolar Deep Water (CDW) fluxes and ocean heat content intruding onto the continental shelf and flowing into the ice shelves cavities (Dotto et al., 2019; Jacobs et al., 2011; Pritchard et al., 2012).

https://doi.org/10.5194/egusphere-2025-3149
Preprint. Discussion started: 25 July 2025

Melting ice shelves can explain about 60% of the biomass variance between all Antarctic polynyas, suggesting that they are the primary supplier of dissolved iron (dFe) to coastal polynyas (Arrigo et al., 2015), and can directly or indirectly contribute to regional marine productivity (Bhatia et al., 2013; Gerringa et al., 2012; Hawkings et al., 2014; Herraiz-Borreguero et al., 2016). The strong melting of the ice shelves can release significant quantities of freshwater (Biddle et al., 2017), resulting in a strong overturning within the ice shelves cavity, called the meltwater pump (St-Laurent et al., 2017). Modelling efforts have identified both resuspended Fe-enriched sediments and CDW entrained to the surface by the meltwater pump as the two primary sources of dFe to coastal polynyas, providing up to 31% of the total dFe, compared to 6% for direct ice shelves input (Dinniman et al., 2020; St-Laurent et al., 2017). Other drivers such as sea-ice coverage (and associated increases in light and dFe availability when sea ice retreats), or winds have also been shown to impact primary productivity in polynyas (Park et al., 2019; Park et al., 2017; Vaillancourt et al., 2003).

The key question of how glacial meltwater variability may impact biological productivity in the ASE has previously been raised during the ASPIRE program (Yager et al., 2012). During the expedition, a significant supply of melt-laden iron-enriched seawater to the central euphotic zone of the ASP was observed, potentially explaining why this area is the most biologically productive in Antarctica (Randall-Goodwin et al., 2015; Sherrell et al., 2015). Other studies in the western Antarctic peninsula and east Antarctica showed that the meltwater pump process was also responsible for natural Fe supply to the surface, increasing primary productivity (Cape et al., 2019; Tamura et al., 2022).

In this study, we investigate the long-term relationship between the main environmental factors of the ASE and the surface biological productivity, with a focus on ice shelves melting. A demonstrated relationship between glacial melt and phytoplankton growth would have far-reaching consequences for regional productivity in coastal Antarctica, and possibly offshore, over the coming decades under expected climate change scenarios (Meredith et al., 2019). We test the hypothesis that changes in glacial melt are linked to the surface ocean primary productivity variability observed over the last two decades. We use a combination of satellite

https://doi.org/10.5194/egusphere-2025-3149
Preprint. Discussion started: 25 July 2025

(ocean color and ice shelf melting rate), climate re-analysis, and model data spanning 1998 to 2017.

2. Materials and Methods

2.1 Study area and polynya mapping

We focus on the PIP and ASP in West Antarctica (Fig. 1). Polynya boundaries were determined using a 15% sea-ice concentration (SIC) mask (Moreau et al., 2015; Stammerjohn et al., 2008) for every 8-day period from June 1998 to June 2017 to accurately represent the size of the polynya through time.

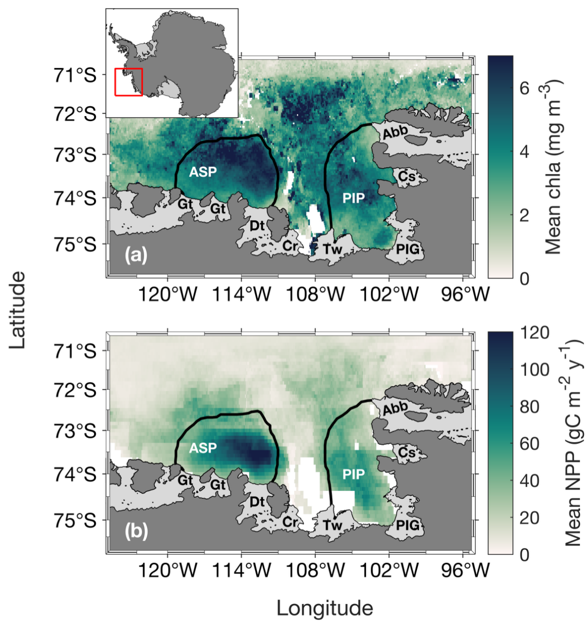

Fig. 1. Spatial distribution of (a) annual surface chl*a* during the bloom and (b) net primary productivity (NPP) climatology (1998 – 2017) for the Amundsen (ASP) and Pine Island (PIP) polynyas. The black lines represent the climatological summer polynya boundaries. The dark grey area is mainland Antarctica. Light grey areas indicate floating ice shelves and glaciers:

https://doi.org/10.5194/egusphere-2025-3149
Preprint. Discussion started: 25 July 2025

Abbot (Abb), Cosgrove (Cs), Pine Island Glacier (PIG), Thwaites (Tw), Crosson (Cr), Dotson (Dt) and Getz (Gt).

2.2 Satellite ocean surface chlorophyll-*a* and net primary productivity

We obtained level-3 satellite surface chlorophyll-*a* (chl*a*) concentration with spatial and temporal resolution of 0.04° and 8 days from the European Space Agency (ESA) Globcolor project (https://www.globcolour.info/). We used standard Case 1 water merged products consisting of the Sea-viewing Wide Field-of-view (SeaWiFS), Medium Resolution Imaging Spectrometer (MERIS), Moderate Resolution Imaging Spectroradiometer (MODIS-A) and Visible Infrared Imaging Suite sensors (VIIRS).

We estimated phytoplankton bloom phenology metrics following the Kauko et al. (2021) method. Firstly, we applied a spatial 3x3 pixels median filter to reduce gaps in missing data. Then, if a pixel was still empty, we applied the average chl*a* of the previous and following week to fill the data gap. Data were smoothed using a 4-point moving median (representing a month of data). For each pixel, the threshold for the bloom detection was based on 1.05 times the annual median. The threshold method is frequently used (Racault et al., 2012; Siegel et al., 2002) and proven reliable at higher latitudes (Marchese et al., 2017; Soppa et al., 2016; Thomalla et al., 2017). We then determined 5 main bloom metrics. The bloom start is defined as the day where chl*a* first exceeds the threshold for at least 2 consecutive 8-day periods. Conversely, the bloom end is the day where chl*a* first falls below the threshold for at least 2 consecutive 8-day periods. The bloom duration is the time elapsed between bloom start and bloom end. The bloom mean chl*a* and bloom max chl*a* are respectively the average and maximum chl*a* value calculated during the bloom. Each year is centered around austral summer, from June 10th year n (day 1) to June 9th year $n+1$ (day 365 or 366). We also averaged our 8-day data to monthly data to perform a spatial correlation analysis (see section 2.6).

Eight-day satellite derived Net Primary Productivity (NPP) data with 1/12° spatial resolution, spanning 1998 - 2017 using the Vertically Generalized Production Model (Behrenfeld & Falkowski, 1997) were obtained from the Oregon State University website. SeaWiFS-based NPP data span 1998 - 2009, MODIS-based data span 2002 - 2017. To increase spatial and temporal coverage, we averaged SeaWiFS and MODIS from 2002 to 2009, where there was valid data for both in a pixel. NPP data were also monthly averaged and used to compare with chl*a* spatial and temporal patterns.

We caution that our study focuses on surface productivity, and satellites cannot detect under-ice phytoplankton and sea-ice algal blooms, therefore likely underestimating total primary productivity (Ardyna et al., 2020; Boles et al., 2020).

2.3 Ice shelves volume flux

We used the latest ice shelf basal melt rate estimates from Paolo et al (2023). These estimates are derived from satellite radar altimetry measurements of ice shelves height, and produced on a 3 km grid every 3 months, with an effective resolution of ~5 km. For this study, our basal melt record spans June 1998 to June 2017. We calculated ice shelves volume flux rate for every gridded cell by multiplying the basal melt rate by the cell area. Data were summed for each ice shelf for a 3-month period. A 5-point (15 months) running mean was applied to reduce noise, such as spurious effects induced by seasonality on radar measurements over icy surfaces (Paolo et al., 2016), and data were temporally averaged from October to March to match the SO phytoplankton growth season (Arrigo et al., 2015), providing yearly mean values. The Abbot, Cosgrove, Thwaites, Pine Island Glacier (PIG), Crosson, Dotson and Getz ice shelves were used to calculate a single total meltwater volume flux (TVF) for the ASE to investigate the link with surface chl*a*. We also investigated the relationship between each polynyas' productivity and their closest ice shelf. The Abbot, Cosgrove, PIG and Thwaites ice shelves were used to calculate the flux rate in the PIP (TVFpip) while the Thwaites, Crosson, Dotson and Getz ice shelves were chosen for the ASP (TVFasp). The Thwaites was used in both due to its central position between the two polynyas.

2.4 Simulated dFe distribution

https://doi.org/10.5194/egusphere-2025-3149
Preprint. Discussion started: 25 July 2025

Spatial distributions of dFe from different sources in the embayment were investigated from Dinniman et al. (2020) model output. The model used is a Regional Ocean Modelling System (ROMS) model, with a 5 km horizontal resolution and 32 terrain following vertical layers and includes sea-ice dynamics, as well as mechanical and thermodynamic interaction between ice shelves and the ocean. The model time run spans seven years and simulates fourteen different tracers to understand dFe supply across the entire Antarctic coastal zone, with the last two years simulating biological uptake. For the purpose of this study, we only use four different dFe sources/tracers in the ASE: ice shelf melt, CDW, sediments and sea ice. Each tracer estimation is independent from each other, meaning that one source does not affect the other, and they have the same probability for biological uptake by phytoplankton. That is, dFe from all sources can equally be taken up by phytoplankton. This is parametrized in the model as all iron molecules being bound to a ligand and therefore remaining in solution in a bioavailable form. For a detailed and complete explanation of the model, see Dinniman et al. (2020).

2.5 Other environmental parameters

We used SIC data spanning June 1998 to June 2017 from the National Snow and Ice Data Center (Cavalieri et al., 1996). The data are Nimbus-7 SMMR and SSMI/SSMIS passive microwave daily SIC with 25 km spatial resolution. We computed the sea-ice retreat (IRT) and open water period (OWP) metrics using a 15% threshold (Stammerjohn et al., 2008). Daily data were monthly averaged to perform a spatial correlation analysis (see section 2.6).

We collected monthly level-4 Optimum Interpolation Sea Surface Temperature (OISST.v2) 0.25° high resolution dataset from the National Oceanic and Atmospheric Administration (Banzon et al., 2016). Using this dataset compared to others has been proven to be the most suitable for our region of interest (Yu et al., 2023).

We obtained monthly Photosynthetically Available Radiation (PAR) from the same Globcolour project at the same spatial and temporal resolution (0.04° and 8 days) as chl*a*.

We used monthly averaged ERA5 reanalysis of zonal (u) and meridional (v) surface wind speed at 10 m above the surface (Hersbach et al., 2020).

2.6 Statistical analysis

Because some of our data were not normaly distributed, we consistently applied nonparametric tests throughout our statistical analysis. A Mann-Kendall test was performed to detect linear trends in chl*a* and NPP. A two-tailed non-parametric Spearman correlation metric (*p*) was calculated to investigate the relationship between chl*a*, NPP, and glacial meltwater, as well as between phytoplankton and sea-ice phenology metrics. A two-tailed Mann-Whitney test was performed to detect any significant mean differences for chl*a* and sea-ice phenology metrics between the two polynyas. A monthly spatial correlation was tested between SIC, winds, chl*a*, NPP, SST, and PAR after removing the seasonality for each parameter. As well, a yearly spatial correlation between chl*a*, NPP and TVF was performed. The relationships between chl*a* concentration, NPP and environmental factors were explored using a Principal Component Analysis (PCA). Every statistical test was run with a 95% (p-value < 0.05) confidence level. Our study spans 1998-2017. We are constrained by the start of satellite ocean color data (1998) and the end of the ice shelf basal melt rate record (2017) from Paolo et al (2023).

3. Results

3.1 Glacial melt and chl*a* variability

The annual climatology maps reveal substantially higher chl*a* concentration and NPP in the ASP compared to the PIP (Fig. 1). During the bloom period, chl*a* concentration is also higher in the ASP on average compared to the PIP (ASP = 5.21 ± 1.29 mg m^{-3} ; PIP = 3.69 ± 1.11 mg m^{-3}, Fig. 2b and Table T1, p-value < 0.01). The chl*a* concentration starts increasing in mid-November to reach its average earlier in the PIP than the ASP. At its peak, chl*a* in the ASP is 6.49 mg m^{-3} and 4.94 mg m^{-3} in the PIP (Fig. 2a). When looking at polynya area integrated values (concentration multiplied by area gives units of mg m^{-1}), chl*a* is significantly higher in the ASP than in the PIP, and increases with the polynya area (Figs. S1 and S2). NPP is also significantly

https://doi.org/10.5194/egusphere-2025-3149
Preprint. Discussion started: 25 July 2025

higher in the ASP than in the PIP (1.88 ± 1.12 TgC y^{-1} vs 0.85 ± 0.86 TgC y^{-1}, p-value = 0.004, Fig. S3). No significant interannual trends in mean chl*a* and NPP during the bloom are observed for either polynya (Fig. 2b, Fig. S3, p-value > 0.1).

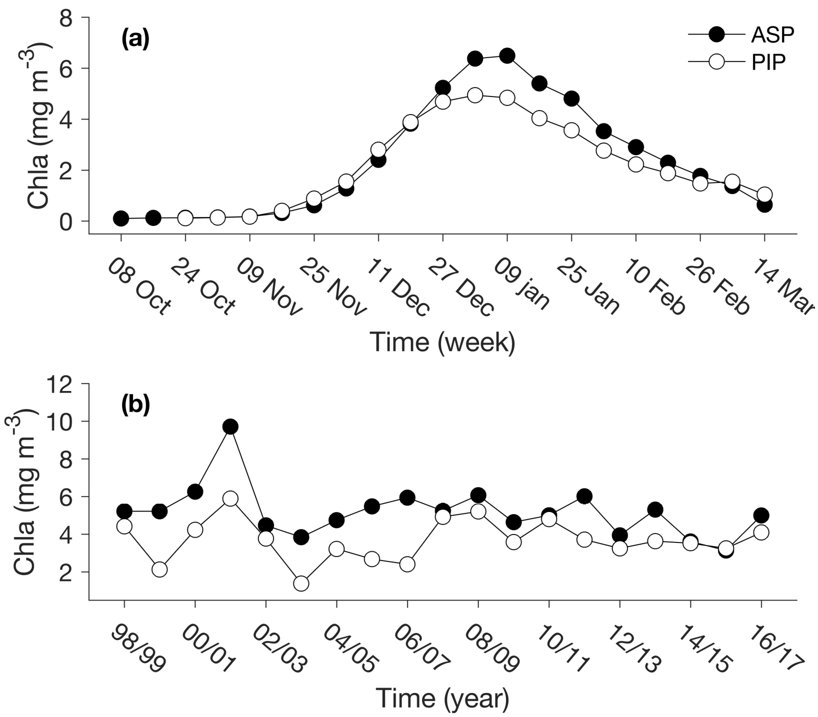

Fig. 2. (a) Weekly chlorophyll-*a* (chl*a*) climatology (1998-2017) for ASP (filled circles) and PIP (open circles). (b) Bloom mean chl*a* time series of ASP (filled circles) and PIP (open circles). The relationship between chl*a* (in mg m^{-3} and mg m^{-1}) and the polynya size is shown in Fig. S2.

The variability in TVF is statistically uncorrelated with surface chl*a* concentration and NPP in both polynyas from 1998 to 2017 (Fig. 3; Fig. S4). However, the relationship becomes strongly significant in the ASP for both mean and max chl*a* when we remove the chla outlier in 2001/02 (red data point, Figs. 3a-b), although not for NPP (Figs S4a-b). The positive relationship implies that surface chl*a* in the ASP is higher when more glacial meltwater is delivered to the embayment. No strong relationships are observed in the PIP between TVF, surface chl*a* and NPP

https://doi.org/10.5194/egusphere-2025-3149
Preprint. Discussion started: 25 July 2025

(Figs. 3c-d; Figs S4c-d). When fluxes from individual glaciers are considered, PIP chl*a* does not correlate with Abbot, Cosgrove, PIG, Thwaites or TVFpip fluxes (Table 1). On the other hand, ASP chl*a* shows strong relationships with TVFasp and the Dotson ice shelf (Table 1). Note that all ice shelves become significantly correlated with mean and max chl*a* when the 2001/02 year is removed. Note that all ice shelves become significantly correlated with mean and max chl*a* when the 2001/02 year is removed. There were no statistically significant relationships between individual ice shelves and NPP in both polynyas. On the other hand, ASP chl*a* shows strong relationships TVFasp (Table 1). Spatially, the mean and max chl*a* are strongly correlated with TVF in the central-eastern part of the ASP, in front of the Dotson ice shelf (Figs. 4a-b), where a positive relationship with NPP is also observed (Fig. 4c), although not significant.

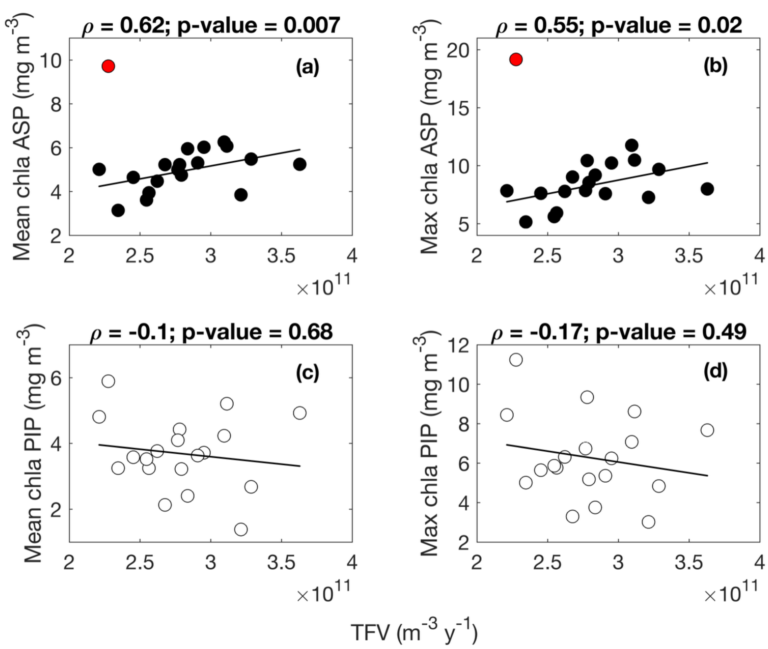

Fig. 3. Scatter plots of mean and max surface chlorophyll-*a* (chl*a*) with TVF for (a-b) the ASP and (c-d) the PIP from 1998 to 2017. The fitted lines and statistics exclude the 2001/02 year (red outlier) for the ASP regressions. If all data is considered, the relationships between mean chl*a*, max chl*a* and TFV in the asp are not significant. TVF is an annual integral representing the sum of all ice shelves (see methods section) for the ASE.

https://doi.org/10.5194/egusphere-2025-3149
Preprint. Discussion started: 25 July 2025

Table 1. Statistical summary of the relationships between volume flux metrics and surface chlorophyll-*a* (chl*a*). The * marks a significant (p-value < 0.05) relationship.

	ASP				PIP			
	Mean chl*a*		Max chl*a*		Mean chl*a*		Max chl*a*	
	rho	p-value	rho	p-value	rho	p-value	rho	p-value
Abbot	/	/	/	/	0.09	0.73	-0.04	0.88
Cosgrove	/	/	/	/	-0.32	0.18	-0.46	0.05
PIG	/	/	/	/	-0.04	0.88	-0.13	0.61
Thwaites	0.16	0.52	0.11	0.66	0.12	0.63	0.09	0.7
Crosson	0.43	0.07	**0.50**	**0.03***	/	/	/	/
Dotson	**0.47**	**0.04***	**0.51**	**0.03***	/	/	/	/
Getz	0.37	0.12	0.43	0.07	/	/	/	/
TVFasp	0.42	0.07	**0.66**	**0.05***	/	/	/	/
TVFpip	/	/	/	/	0.09	0.73	-0.04	0.88

https://doi.org/10.5194/egusphere-2025-3149
Preprint. Discussion started: 25 July 2025

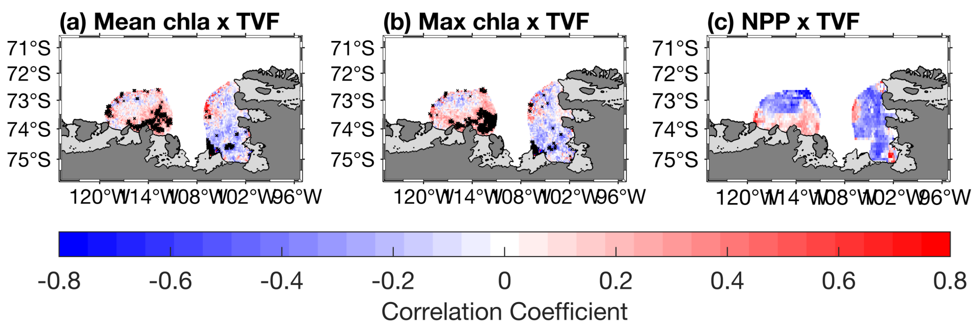

Fig. 4. Spatial correlation maps between total volume flux (TVF) and (a) surface mean chlorophyll-*a* (chl*a*), (b) surface max chl*a* and (c) net primary productivity (NPP) (n=19). The black crosses represent significant correlation at 95% confidence level. Data outside of the summer climatological polynyas boundaries were masked out.

3.2 Simulated dFe sources distribution

The modelled spatial distributions of surface dFe sources are presented in Fig. 5. On average, the smallest dFe source in the embayment is from the ice shelves (Fig. 5a), with a maximum concentration between the Thwaites and Dotson ice shelves. The dFe from sea ice is slightly higher than from ice shelves and similar over the two polynyas, and is higher near the sea-ice margin (Fig. 5b). The dFe from CDW is also higher between the Thwaites and Dotson (Fig. 5c). Sediment is the dominant dFe source (Fig. 5d). Its distribution spreads from 108°W to the western part of the Getz ice shelf. The highest sediment concentration is found along the coast and inside the ASP. On polynya-wide average basis, the sediment reservoir contributes significantly more to total dFe in the ASP (58.3%, 0.13nM) compared to sea ice (16.5%, 0.04nM), CDW (13.5%, 0.03nM) and ice shelves (11.7%, 0.03nM). In the PIP, the contribution of sediments is still significantly higher (41.2%; 0.08nM) but lower than the ASP and the contribution gap with the other sources decreases. The CDW and sea ice contribute 22.5% (0.04nM) and 18.9% (0.035nM) to the dFe pool respectively, while ice shelves are still the smallest sources at 14.5% (0.03nM) in the PIP.

https://doi.org/10.5194/egusphere-2025-3149
Preprint. Discussion started: 25 July 2025

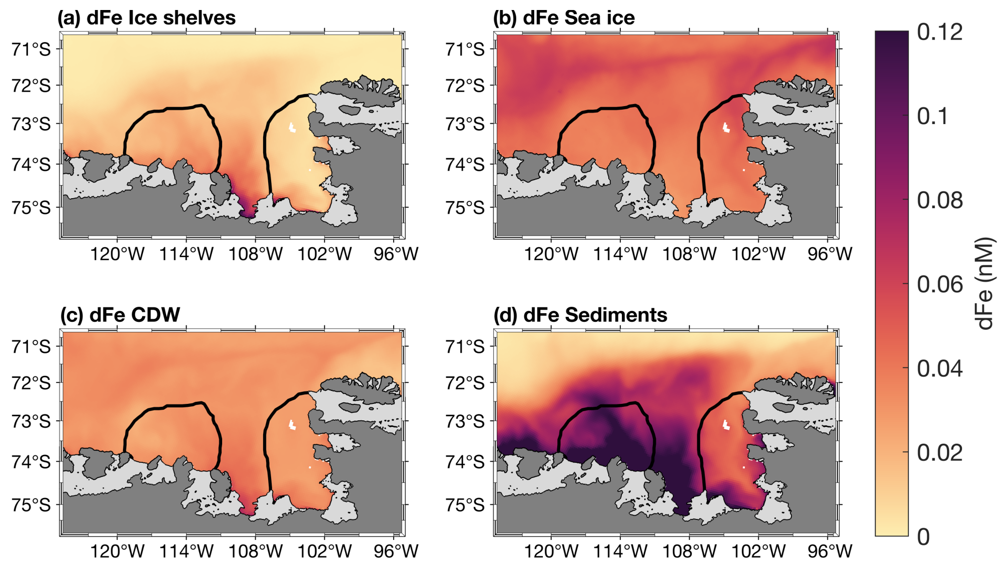

Fig. 5. Two-years top-100m averaged spatial distribution of surface dissolved iron (dFe) contribution from (a) ice shelves, (b) sea ice, (c) circumpolar deep water and (d) sediments simulated by the model from Dinniman et al. (2020). The black lines represent the climatological summer polynya boundaries.

3.3 Environmental parameters, chl*a* and NPP variability

During the phytoplankton growth season (October-March), SIC is spatially significantly anticorrelated to the meridional winds speed in both polynyas (Fig. 6a). Chl*a* is significantly positively correlated with SST in the central-eastern ASP, and the whole PIP (Fig. 6b), but weakly with PAR in both polynyas (Fig. 6c). Finally, PAR and SST are positively linked in both central polynyas, albeit not significantly (Fig. 6d). We note that similar spatial relationships are observed when NPP is correlated with SST and PAR. (Fig. S5).

https://doi.org/10.5194/egusphere-2025-3149
Preprint. Discussion started: 25 July 2025

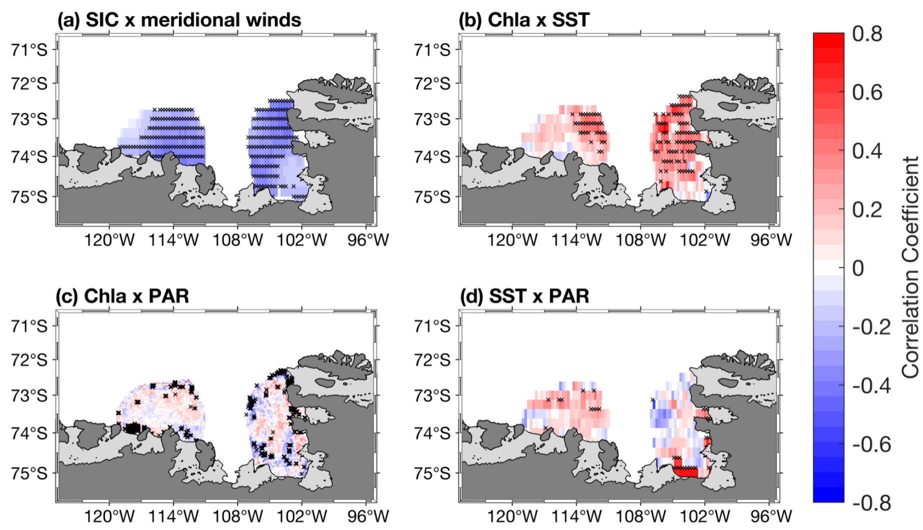

Fig. 6. Spatial correlation maps between sea-ice concentration (SIC) and (a) meridional winds. Spatial correlation maps between chlorophyll-*a* (chl*a*) concentration (mg m^{-3}) and (b) sea surface temperature (SST), (c) photosynthetically available radiation (PAR). (d) Spatial correlation between PAR and SST. Data span 1998 – 2017 from October to March (n=114). The black crosses represent significant correlation at 95% confidence level. Seasonality was removed from the data before preforming the correlation. Data outside of the summer climatological polynyas boundaries were masked out.

Regarding the phenology, the bloom start is positively correlated to IRT and negatively with OWP in the ASP, although not significantly with the OWP (Table 2). This means that the bloom starts earlier and later as IRT does, and that longer OWP and earlier bloom starts are correlated with earlier ice retreat. The bloom mean and bloom max chl*a* are not correlated with either IRT and OWP in the ASP. In the PIP, all metrics are significantly related to each other, except for PAR and OWP (Table 2). That is, the bloom start is positively correlated with IRT and negatively with OWP, while the bloom duration, mean chl*a*, max chl*a* concentrations and NPP are negatively linked to the IRT and positively with OWP. SST and PAR are negatively correlated to IRT, while OWP is only significantly positively correlated to SST. IRT and OWP are significantly related in the PIP.

https://doi.org/10.5194/egusphere-2025-3149
Preprint. Discussion started: 25 July 2025

Table 2. Statistical summary of the relationships between the phytoplankton and sea-ice phenology metrics. The * marks a significant (p-value < 0.05) relationship. IRT = ice retreat time, OWP = open water period, NPP = net primary productivity, SST = sea surface temperature, PAR = photosynthetically available radiation.

	Amundsen Sea polynya				Pine Island polynya			
	IRT		OWP		IRT		OWP	
	rho	p-value	rho	p-value	rho	p-value	rho	p-value
Bloom start	**0.51**	**0.04***	-0.43	0.08	**0.56**	**0.02***	**-0.48**	**0.04***
Bloom duration	-0.12	0.60	0.09	0.72	**-0.56**	**0.02***	**0.59**	**0.01***
Bloom mean	0.20	0.44	-0.35	0.16	**-0.67**	**0.003***	**0.50**	**0.04***
Bloom max	0.25	0.32	-0.36	0.14	**-0.65**	**0.005***	**0.52**	**0.03***
NPP	**-0.55**	**0.02***	0.45	0.05	**-0.72**	**0.001***	**0.52**	**0.02***
SST	-0.07	0.79	-0.03	0.91	**-0.57**	**0.02***	**0.52**	**0.03***
PAR	-0.11	0.66	0.09	0.71	**-0.62**	**0.007***	0.38	0.13

We explore the relationships between phytoplankton bloom phenologies and their potential environmental drivers by conducting a multivariate PCA for both polynyas (Fig. 7). In the ASP (Fig. 7a), the first two principal components explain 58.1% of the total variance (Dim1: 37.9%, Dim2: 20.2%). NPP in the ASP is closely associated with PAR and BD, indicating that light availability and bloom duration are primary drivers of production. On the other hand environmental vectors such as TVFall and TVFasp projected more strongly onto Dim2 with the bloom mean chl*a*, indicating that meltwater input may influence surface chl*a* interannual variability, and is less directly tied to NPP. We note that when the 2001/02 summer is removed, the relationship between TVFasp and TVFall becomes much stronger with the bloom mean chl*a* (Fig. S7a) and is slightly anti correlated to SST. In the PIP (Fig. 7b), the first two components accounted for 66.9% of the total variance (Dim1: 48.2%, Dim2: 18.7%). Compared to the ASP,

https://doi.org/10.5194/egusphere-2025-3149
Preprint. Discussion started: 25 July 2025

both NPP and BM clustered strongly with BD and PAR. Additionally, OWP and SST aligned along Dim1, suggesting that physical conditions might play a stronger structuring role in PIP compared to the ASP. In contrast, TVFall and TVFpip stand alone and align more strongly with Dim2, suggesting a less dominant influence of meltwater on the system bloom mean chl*a* and NPP variability in the PIP.

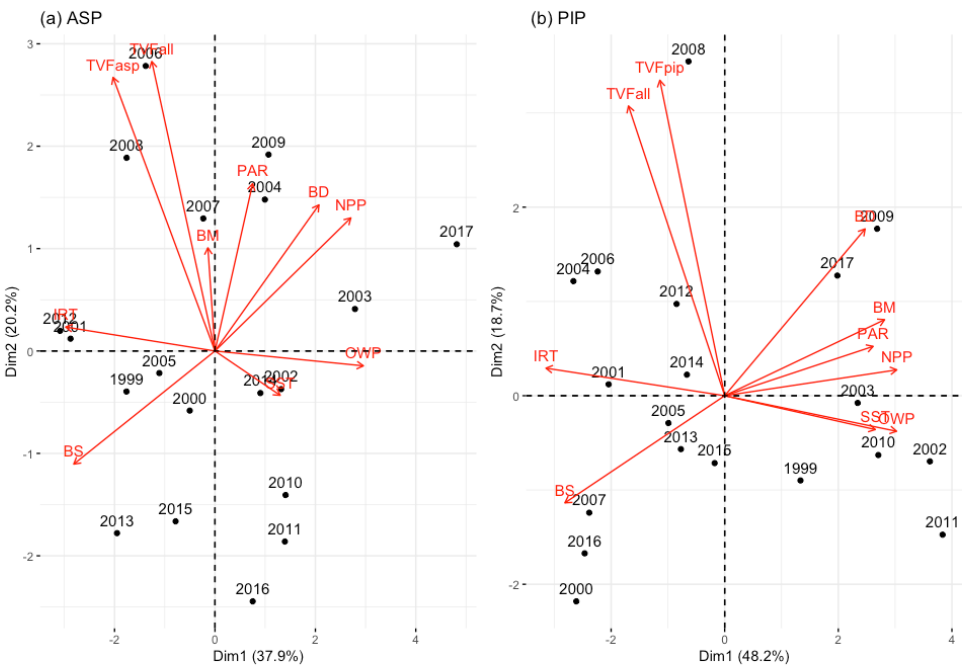

Fig. 7. Principal component analysis biplot of environmental parameters (red) and years (black) for (a) the ASP and (b) the PIP. Same plot is presented in supplementary Figure S7 but removing the 2001/02 anomalous year for the ASP, emphasizing the relationship between total volume fluxes (TVFall, TVFasp) and the bloom mean (BM) in the ASP.

4. Discussion

4.1 Effect of ice shelf meltwater on phytoplankton chl*a* and NPP

https://doi.org/10.5194/egusphere-2025-3149
Preprint. Discussion started: 25 July 2025

The relationship between glacial melt rates and surface chl*a* observed over the last two decades was distinctly different between the two polynyas. In the ASP, we found that enhanced glacial melt translates into higher surface chl*a*, but not with NPP (when removing the anomalous 2001/02 summer; Figs. 3a-b; Fig. S7a). Modelling results (Fig. 5) suggest that sediment from the seafloor is the main source of dFe in the ASP, but this source is also linked to glacial melt. Ice shelf glacial meltwater drives the meltwater pump, which brings up modified CDW (mCDW) and fine-grained subglacial sediments to the surface. This result is in agreement with previous research: Melt-laden modified CDW flowing offshore from the Dotson ice shelf to the central ASP (Sherrell et al., 2015), and resuspended sediments (Dinniman et al., 2020; St-Laurent et al., 2017; 2019) have been identified as significant sources of dFe to be used by phytoplankton. Interestingly, both dFe supplied from ice shelves and CDW are most important in front of the Thwaites and Crosson ice shelves, where the area averaged basal melt rate, and thus likely the area averaged meltwater pumping (Jourdain et al., 2017) are typically strongest in observations (Adusumilli et al., 2020; Rignot et al., 2013) and the modelling (Fig. 5). The year 2001/02 does not stand out as being influenced by any specific parameter in the ASP compared to other years (Fig. 7a; Fig. S7a). The anomalously high surface chl*a* observed during this year, as also reported by Arrigo et al. (2012), may result from exceptional conditions that were not captured by the parameters analysed in our study - for instance, an imbalance in the grazing pressure. Interestingly, surface chl*a* and NPP exhibit contrasting trends when averaged across the polynya. While TVF may explain some of the variance in surface chl*a*, it does not account for the variance in NPP, whether assessed through direct or multivariate relationships. This decoupling between chl*a* and NPP in the ASP suggests that ice shelf meltwaters, while enhancing surface phytoplankton biomass through nutrient delivery, also promote vertical mixing. This mixing deepens the mixed layer, reducing light availability and constraining photosynthetic rates. These rates are influenced by fluctuations in the MLD, even in the presence of high biomass and sufficient macronutrients. Additionally, interannual variability in the composition of the phytoplankton community may further explain these observations. For example, the occasional dominance of the small prymnesiophyte *Phaeocystis antarctica*, a low-efficiency primary producer (Lee et al., 2017), can contribute to high surface chl*a* but relatively modest and decoupled NPP.

https://doi.org/10.5194/egusphere-2025-3149
Preprint. Discussion started: 25 July 2025

In the PIP, we did not find any long-term relationship between the phytoplankton bloom, NPP and glacial meltwater. Variability in ice shelf melt rates may not have the same effect on the surface chl*a* and NPP in the PIP compared to the ASP. Iron delivered from glacial melt process related in the PIP and west of it could accumulate and follow the westward coastal current, towards the ASP (St-Laurent et al., 2017). These sources would include dFe from meltwater pumped CDW, sediments and ice shelves, all of which are higher in front of the Crosson ice shelf, west of the PIP (Fig. 5). With the coastal circulation, this would make dFe supplied by glacial meltwater greater in the ASP, thereby contributing to the higher productivity in the ASP. Recently, subglacial discharge (SGD) was shown to have a different impact on basal melt rate in the ASE polynyas (Goldberg et al., 2023), where PIG had a lot less relative increase in melt with SGD input than Thwaites or Dotson/Crosson. Thus, assuming a direct relationship between meltrate, SGD and dFe sources, the signal in the PIP (fed by PIG melt) will be much weaker than in the ASP (fed by upstream Thwaites, Crosson and local Dotson due to the circulation), which might also explain the discrepancies between the PIP and ASP. The model outputs used here are critical to understand the spatial distribution of dFe in the embayment. They strongly suggest but do not definitively demonstrate the role of dFe in influencing the phytoplankton bloom interannual variability.

Direct observations from Sherrell et al. (2015) showed higher chl*a* in the central ASP while surface dFe was low weeks before the bloom peak. This suggests a continuous supply and consumption of dFe in the area. Considering the long residence time of water masses in both polynyas (about 2 years (Tamsitt et al., 2021)), and the daily dFe uptake by phytoplankton (3-196 pmol l^{-1} d^{-1} (Lannuzel et al., 2023)), we also hypothesise that any dFe reaching the upper ocean from external sources is quickly used and unlikely to remain readily available for phytoplankton in the following spring season.

In recent model simulations with the meltwater pump turned off, Fe becomes the principal factor limiting phytoplankton growth in the ASP (Oliver et al., 2019). However, the transport of Fe-rich glacial meltwater outside the ice shelf cavities and to the ocean surface depends strongly on the local hydrography. While Naveira Garabato et al. (2017) suggested that the glacial meltwater concentration and settling depth outside the ice shelf cavities is controlled by an overturning

https://doi.org/10.5194/egusphere-2025-3149
Preprint. Discussion started: 25 July 2025

circulation driven by instability, others suggest that the strong stratification plays an important role in how close to the surface the buoyant plume of said meltwater can rise (Arnscheidt et al., 2021; Zheng et al., 2021). Therefore, high melting years and greater TVF might not necessarily translate into a more iron-enriched meltwater delivered to the surface outside the ice shelf cavities, close to the ice shelf edge, as rising water masses may be either prevented from doing so, or be transported further offshore in the polynyas where the phytoplankton bloom occurs, before they can resurface (Herraiz-Borreguero et al., 2016).

Although several Fe sources can fuel polynya blooms, and they depend on processes mentioned above, Fe-binding ligands may ultimately set the limit on how much of this dFe stays dissolved in the surface waters (Gledhill & Buck, 2012; Hassler et al., 2019; Tagliabue et al., 2019). Models of the Amundsen Sea (Dinniman et al., 2020, 2023; St-Laurent et al., 2017, 2019) did not include Fe complexation with ligands and assumed a continuous supply of available dFe for phytoplankton. Spatial and seasonal data on Fe-binding ligands along the Antarctic coast remain extremely scarce and their dynamics are poorly understood (see Smith et al. (2022) for a database of publicly available Fe-binding ligand surveys performed south of 50°S). Field observations in the ASP and PIP suggest that the ligands measured in the upwelling region in front of the ice shelves had little capacity to complex any additional Fe supplied from glacial melt. As a consequence, much of the glacial and sedimentary Fe supply in front of the ice shelves could be lost via particle scavenging and precipitation (Thuróczy et al., 2012). This was also recently observed by van Manen et al. (2022) in the ASP. However, within the polynya blooms, Thuróczy et al. (2012) found that the ligands produced by biological activity were capable of stabilising additional Fe supplied from glacial melt, where we observed the highest productivity. The production of ligands by phytoplankton would increase the stock of bioavailable Fe and further fuel the phytoplankton bloom in the polynyas. Model development and sustained field observations on Fe availability, including ligands, are needed to adequately predict how these may impact biological productivity under changing glacial and oceanic conditions, now and in the future.

Overall, the discrepancies observed between the ASP and PIP point to a complex set of ice-ocean-sediment interactions, where several co-occurring processes and differences in

https://doi.org/10.5194/egusphere-2025-3149
Preprint. Discussion started: 25 July 2025

hydrographic properties of the water column influence dFe supply and consequent primary productivity.

4.2 Possible drivers of the difference in phytoplankton surface chl*a* and NPP between the two polynyas

The biological productivity is higher in the ASP than the PIP, consistent with previous studies (Arrigo et al., 2012; Park et al., 2017). In section 4.1, we mentioned the underlying hydrographic drivers of these differences. We related the higher biological productivity in the ASP to a potentially greater supply of iron from melt-laden Fe-enriched mCDW and sediment sources, but this difference in productivity could also be attributed to other local features. The Bear Ridge grounded icebergs (BRI) on the ASP's eastern side (Bett et al., 2020) could add to the overall meltwater pump strength. They can enhance warm CDW intrusions to the ice shelf cavity (Bett et al., 2020), increasing ice shelf melting and subsequent stronger phytoplankton bloom from the meltwater pump activity. These processes are weaker or absent in the PIP. Few sources other than glacial meltwater may influence the bloom in the PIP. For instance, dFe in the euphotic zone can also be sustained by the biological recycling, as shown in the PIP by Gerringa et al. (2020).

Sea ice could also partly explain the difference in chl*a* magnitudes, NPP, and variability between the ASP and PIP. The strong spatial correlation between SIC and meridional winds (Fig. 6a) indicates that southerly winds can export the coastal sea ice offshore and play a significant role in opening the polynyas. In the ASP compared to the PIP, sea ice retreats earlier (IRT = Jan 1st ± 14d vs Jan 18th ± 17d, p-value = 0.003), the open water period is longer (OWP = 61 ± 16d vs 44 ± 22d, p-value < 0.001), and the SIC is lower (Fig. S6c, Table 2). In the ASP, an early sea-ice retreat leads to an earlier bloom start, but the longer open water period is not significantly associated with greater bloom mean and max chl*a* (Table 2). On the other hand in the PIP, an early sea-ice retreat also triggers an early bloom start, but the longer open duration is associated with warmer water, higher bloom mean chl*a*, max chl*a*, and NPP. These results suggest that different processes might drive phytoplankton growth in the two polynyas. In the ASP, it is likely the replenishment of dFe mentioned above that mostly influences the bloom. In the PIP,

https://doi.org/10.5194/egusphere-2025-3149
Preprint. Discussion started: 25 July 2025

the higher SIC can delay the retreat time and shorten the open water season (Table 2; Fig. S6), leading to less light availability and lower phytoplankton productivity compared to the ASP. The significant negative relationship between IRT, PAR, chl*a* and NPP in the PIP (Table 2; Fig. S6) suggests a strong light limitation relief in the polynya. This light limitation hypothesis is further supported by the high correlation between polynya-averaged chl*a* mean with PAR and SST in the PIP across the 19 years of study compared to the lack of correlation in the ASP (Table T2; p-value < 0.01 for all relationships in the PIP). Similar results have been reported by Park et al. (2017). They found that the PIP was dFe replete, potentially from biological recycling (Gerringa et al., 2020), compared to an iron-limited ASP. We hypothesise that the connection between ice shelf meltwater and chl*a* that we found in the ASP is a response to iron input (also observed by Park et al. (2017) during incubation experiments) compared to the PIP, where light and temperature seem to play a more significant role in driving the phytoplankton bloom variability.

Variability in SIC and sea-ice retreat can be influenced by the Amundsen Sea Low (ASL; Hosking et al., 2013; Turner et al., 2016). We therefore also investigated its potential role on sea-ice variability. We found on average weak spatial negative relationships between SIC and ASL latitude, longitude, mean sector and actual central pressure in both polynyas during the growing seasons (Fig. S8), and only slightly significant in the eastern PIP. The weak relationships might be owing to the seasonal variation of the ASL, where its position largely varies during summer, and its impact in shaping coastal sea ice is also greater during winter and autumn in the Amundsen-Bellingshausen region (Hosking et al., 2013). The lack of strong significant relationships overall does not allow us to conclude that the ASL plays an important role in shaping the coastal polynyas landscape and influencing chl*a* variability.

4.3 Limitations and future directions

While it seems reasonable that the higher ASP productivity could be driven by more iron delivered through a stronger meltwater pump downstream of the PIP, our data cannot confirm this hypothesis. To accurately understand the role of iron through the meltwater pump process, we would need to quantify the fraction of meltwater and glacial modified water (mix of CDW and ice shelf meltwater) reaching the ocean surface, together with the iron content. Obtaining

https://doi.org/10.5194/egusphere-2025-3149
Preprint. Discussion started: 25 July 2025

this information is challenging over the decadal time scales considered and the method used in our study. Here, our intention was to provide insights into the potential drivers of our results, and highlight the benefit of remote sensing in this poorly observed environment. Our work directly aligns with Pan et al. (2025), who investigated the long-term relationship between sea surface glacial meltwater and satellite surface chl*a* in the Western Antarctic Peninsula, and found a strong relationship between the two parameters, highlighting the importance of glacial meltwater discharge in regions prone to extreme and rapid climate changes.

In multimodel climate change simulations, Naughten et al (2018) showed an increase of ice shelves melting up to 90% on average, attributed to more warm CDW on the shelf, due to atmospherically driven changes in local sea-ice formation. More recently, Dinniman et al. (2023) also highlighted the impact of projected atmospheric changes on Antarctic ice sheet melt. They showed that strengthening winds, increasing precipitation and warmer atmospheric temperatures will increase heat advection onto the continental shelf, ultimately increasing basal melt rate by 83% by 2100. Compared to present climate simulations, their simulation showed a 62% increase in total dFe supply to shelf surface waters, while basal melt driven overturning Fe supply increased by 48%. The ice shelf melt and overturning contributions varied spatially, increasing in the Amundsen-Bellingshausen area and decreasing in East Antarctica. This implies that, under future climate change, phytoplankton productivity could show stronger spatial asymmetry around Antarctica. The increasing melting and thinning of ice shelves will eventually result in more numerous calving events and drifting icebergs (Liu et al., 2015). Model simulations stressed the importance of ice shelves and icebergs in delivering dFe to the SO (Death et al., 2014; Person et al., 2019), increasing offshore productivity. As Fe will likely be replenished and sufficient from increasing melting in coastal areas, it is possible that the system will shift from Fe-limited to being limited by nitrate, silicate, or even manganese (Anugerahanti & Tagliabue, 2024). while offshore SO productivity will likely remain Fe-dependent (Oh et al., 2022).

5. Conclusions

Using spatial and multivariate approaches, our study explored the variability of surface chl*a* and NPP in the Amundsen Sea polynyas over the last two decades, with a focus on the main

https://doi.org/10.5194/egusphere-2025-3149
Preprint. Discussion started: 25 July 2025

environmental characteristics of the ASE. We found a potential strong relationship between ice shelf melting and surface chl*a* in the ASP, which becomes stronger when the anomalous 2001/02 summer was removed, a result in agreement with the ASPIRE field studies and previous satellite analyses. On the other hand, we did not find clear evidence of such a relationship in the PIP, where light, sea surface temperature and open water availability seem more important. The differences between the polynyas may lie in hydrographic properties, or the use of satellite remote sensing itself, which cannot tell us about processes such as Fe supply, bioavailability and phytoplankton demand. To gain greater insight, we referred to model simulations that showed the spatial variability in the magnitude of iron sources. Our results call for sustained *in situ* observations (e.g. moorings equipped with trace-metal clean samplers, and physical sensors to better understand year-to-year water mass meltwater fraction and properties) to elucidate these long-term relationships. Satellite observations are a powerful tool to investigate the relationship between glacial ice meltwater and biological productivity on such time scales, which has until now relied almost exclusively on field observations and modelling. Using such tools, we showed how the relationship between phytoplankton and the environment varies spatially and temporally across 19 years.

Appendices

No appendices are related to the manuscript.

Data availability

Satellite surface chlorophyll-*a* and photosynthetically available radiation were downloaded from https://www.globcolour.info/. Sea surface temperature (Banzon et al., 2016) can be found here https://psl.noaa.gov/data/gridded/data.noaa.oisst.v2.highres.html. Wind re-analysis data (Hersbach et al., 2020) are available at https://cds.climate.copernicus.eu/cdsapp#!/dataset/10.24381/cds.f17050d7?tab=form. Sea-ice concentration (Cavalieri et al., 1996) was obtained from https://nsidc.org/data and Net Primary productivity (Behrenfeld & Falkowski, 1997) was downloaded from http://sites.science.oregonstate.edu/ocean.productivity/index.php. Circumpolar surface model output from Dinniman et al (2020) can be found at https://www.bco-dmo.org/dataset/782848.

https://doi.org/10.5194/egusphere-2025-3149
Preprint. Discussion started: 25 July 2025

The Amundsen Sea Low index (Hosking et al., 2016) data are available at http://scotthosking.com/asl_index.

Author contributions

GL conceptualised and led the study; MSD provided the dissolved iron model output. All authors were involved in the interpretation of the results, the revision, and the writing of the final version of the paper.

Competing interest

We declare having no competing interests.

Acknowledgments

We would like to thank the University of Tasmania, the Australian Research Council (ARC) Centre of Excellence for Climate Extremes (CE170100023), and the Australian Centre for Excellence in Antarctic Science (ACEAS; SR200100008) for financial support. Delphine Lannuzel is funded by the ARC through a Future Fellowship (L0026677). Sebastien Moreau received funding from the Research Council of Norway (RCN) for the project "I-CRYME: Impact of CRYosphere Melting on Southern Ocean Ecosystems and biogeochemical cycles" (grant number 335512) and for the Norwegian Centre of Excellence "iC3: Center for ice, Cryosphere, Carbon and Climate" (grand number 332635). Michael Dinniman was supported by the U.S National Science Foundation grant OPP-1643652. We are also grateful to Will Hobbs, Rob Massom and Patricia Yager for their knowledgeable input. We thank Vincent Georges for some preliminary work as part of his masters' internship. We are very grateful to Fernando S. Paolo for his early input and help with the ice shelf meltwater dataset. We thank the data providers mentioned in the methods section for making their data available and free of charge.

Financial support

All financial support were mentioned in the Acknowledgment section.

References

Adusumilli, S., Fricker, H. A., Medley, B., Padman, L., & Siegfried, M. R. (2020). Interannual variations in meltwater input to the Southern Ocean from Antarctic ice shelves. *Nature Geoscience*, *13*(9), 616–620. https://doi.org/10.1038/s41561-020-0616-z

Anugerahanti, P., & Tagliabue, A. (2024). Response of Southern Ocean Resource Stress in a Changing Climate. *Geophysical Research Letters*, *51*(10), e2023GL107870. https://doi.org/10.1029/2023GL107870

Ardyna, M., Mundy, C. J., Mayot, N., Matthes, L. C., Oziel, L., Horvat, C., et al. (2020). Under-Ice Phytoplankton Blooms: Shedding Light on the "Invisible" Part of Arctic Primary Production. *Frontiers in Marine Science*, *7*. https://doi.org/10.3389/fmars.2020.608032

Arnscheidt, C. W., Marshall, J., Dutrieux, P., Rye, C. D., & Ramadhan, A. (2021). On the Settling Depth of Meltwater Escaping from beneath Antarctic Ice Shelves. *Journal of Physical Oceanography*, *51*(7), 2257–2270. https://doi.org/10.1175/JPO-D-20-0286.1

Arrigo, K. R., Lowry, K. E., & van Dijken, G. L. (2012). Annual changes in sea ice and phytoplankton in polynyas of the Amundsen Sea, Antarctica. *Deep Sea Research Part II: Topical Studies in Oceanography*, *71–76*, 5–15. https://doi.org/10.1016/j.dsr2.2012.03.006

Arrigo, K. R., & van Dijken, G. L. (2003). Phytoplankton dynamics within 37 Antarctic coastal polynya systems. *Journal of Geophysical Research: Oceans*, *108*(C8). https://doi.org/10.1029/2002JC001739

Arrigo, K. R., van Dijken, G. L., & Strong, A. L. (2015). Environmental controls of marine productivity hot spots around Antarctica. *Journal of Geophysical Research: Oceans*, *120*(8), 5545–5565. https://doi.org/10.1002/2015JC010888

Arrigo, K. R., Worthen, D., Schnell, A., & Lizotte, M. P. (1998). Primary production in Southern Ocean waters. *Journal of Geophysical Research: Oceans*, *103*(C8), 15587–15600. https://doi.org/10.1029/98JC00930

Banzon, V., Smith, T. M., Chin, T. M., Liu, C., & Hankins, W. (2016). A long-term record of blended satellite and in situ sea-surface temperature for climate monitoring, modeling and environmental studies. *Earth System Science Data*, *8*(1), 165–176. https://doi.org/10.5194/essd-8-165-2016

https://doi.org/10.5194/egusphere-2025-3149
Preprint. Discussion started: 25 July 2025

Behrenfeld, M. J., & Falkowski, P. G. (1997). Photosynthetic rates derived from satellite-based chlorophyll concentration. *Limnology and Oceanography*, *42*(1), 1–20. https://doi.org/10.4319/lo.1997.42.1.0001

Bett, D. T., Holland, P. R., Naveira Garabato, A. C. N., Jenkins, A., Dutrieux, P., Kimura, S., & Fleming, A. (2020). The Impact of the Amundsen Sea Freshwater Balance on Ocean Melting of the West Antarctic Ice Sheet. *Journal of Geophysical Research: Oceans*, *125*(9). https://doi.org/10.1029/2020JC016305

Bhatia, M. P., Kujawinski, E. B., Das, S. B., Breier, C. F., Henderson, P. B., & Charette, M. A. (2013). Greenland meltwater as a significant and potentially bioavailable source of iron to the ocean. *Nature Geoscience*, *6*(4), 274–278. https://doi.org/10.1038/ngeo1746

Biddle, L. C., Heywood, K. J., Kaiser, J., & Jenkins, A. (2017). Glacial Meltwater Identification in the Amundsen Sea. *Journal of Physical Oceanography*, *47*(4), 933–954. https://doi.org/10.1175/JPO-D-16-0221.1

Boles, E., Provost, C., Garçon, V., Bertosio, C., Athanase, M., Koenig, Z., & Sennéchael, N. (2020). Under-Ice Phytoplankton Blooms in the Central Arctic Ocean: Insights From the First Biogeochemical IAOOS Platform Drift in 2017. *Journal of Geophysical Research: Oceans*, *125*(3), e2019JC015608. https://doi.org/10.1029/2019JC015608

Boyd, P. W., Jickells, T., Law, C. S., Blain, S., Boyle, E. A., Buesseler, K. O., et al. (2007). Mesoscale Iron Enrichment Experiments 1993-2005: Synthesis and Future Directions. *Science*, *315*(5812), 612–617. https://doi.org/10.1126/science.1131669

Cape, M. R., Vernet, M., Pettit, E. C., Wellner, J., Truffer, M., Akie, G., et al. (2019). Circumpolar Deep Water Impacts Glacial Meltwater Export and Coastal Biogeochemical Cycling Along the West Antarctic Peninsula. *Frontiers in Marine Science*, *6*. https://doi.org/10.3389/fmars.2019.00144

Cavalieri, D., Parkinson, C., Gloersen, P., & Zwally, H. J. (1996). Sea Ice Concentrations from Nimbus-7 SMMR and DMSP SSM/I-SSMIS Passive Microwave Data, Version 1 [Data set]. NASA National Snow and Ice Data Center DAAC. https://doi.org/10.5067/8GQ8LZQVL0VL

Death, R., Wadham, J. L., Monteiro, F., Le Brocq, A. M., Tranter, M., Ridgwell, A., et al. (2014). Antarctic ice sheet fertilises the Southern Ocean. *Biogeosciences*, *11*(10), 2635–2643. https://doi.org/10.5194/bg-11-2635-2014

https://doi.org/10.5194/egusphere-2025-3149
Preprint. Discussion started: 25 July 2025

Dinniman, M. S., St-Laurent, P., Arrigo, K. R., Hofmann, E. E., & van Dijken, G. L. (2020). Analysis of Iron Sources in Antarctic Continental Shelf Waters. *Journal of Geophysical Research: Oceans*, *125*(5). https://doi.org/10.1029/2019JC015736

Dinniman, M. S., St-Laurent, P., Arrigo, K. R., Hofmann, E. E., & van Dijken, G. L. (2023). Sensitivity of the Relationship Between Antarctic Ice Shelves and Iron Supply to Projected Changes in the Atmospheric Forcing. *Journal of Geophysical Research: Oceans*, *128*(2), e2022JC019210. https://doi.org/10.1029/2022JC019210

Dotto, T. S., Naveira Garabato, A. C. N., Bacon, S., Holland, P. R., Kimura, S., Firing, Y. L., et al. (2019). Wind-Driven Processes Controlling Oceanic Heat Delivery to the Amundsen Sea, Antarctica. *Journal of Physical Oceanography*, *49*(11), 2829–2849. https://doi.org/10.1175/JPO-D-19-0064.1

Gerringa, L. J. A., Alderkamp, A.-C., Laan, P., Thuróczy, C.-E., De Baar, H. J. W., Mills, M. M., et al. (2012). Iron from melting glaciers fuels the phytoplankton blooms in Amundsen Sea (Southern Ocean): Iron biogeochemistry. *Deep Sea Research Part II: Topical Studies in Oceanography*, *71–76*, 16–31. https://doi.org/10.1016/j.dsr2.2012.03.007

Gerringa, L. J. A., Alderkamp, A.-C., Laan, P., Thuróczy, C.-E., de Baar, H. J. W., Mills, M. M., et al. (2020). Corrigendum to "Iron from melting glaciers fuels the phytoplankton blooms in Amundsen Sea (Southern Ocean): iron biogeochemistry" (Gerringa et al., 2012). *Deep Sea Research Part II: Topical Studies in Oceanography*, *177*, 104843. https://doi.org/10.1016/j.dsr2.2020.104843

Gledhill, M., & Buck, K. (2012). The Organic Complexation of Iron in the Marine Environment: A Review. *Frontiers in Microbiology*, *3*. https://doi.org/10.3389/fmicb.2012.00069

Goldblerg, D. N., Twelves, A. G., Holland, P. R.. & Wearing, K. G. (2023). The non-local impact of Antarctic subglacial runoff. *Journal of Geophysical Research: Oceans1 128, e2023JC019823.* https://doi.org/10.1029/2023JC01982

Hassler, C., Cabanes, D., Blanco-Ameijeiras, S., Sander, S. G., Benner, R., Hassler, C., et al. (2019). Importance of refractory ligands and their photodegradation for iron oceanic inventories and cycling. *Marine and Freshwater Research*, *71*(3), 311–320. https://doi.org/10.1071/MF19213

https://doi.org/10.5194/egusphere-2025-3149
Preprint. Discussion started: 25 July 2025

Hawkings, J. R., Wadham, J. L., Tranter, M., Raiswell, R., Benning, L. G., Statham, P. J., et al. (2014). Ice sheets as a significant source of highly reactive nanoparticulate iron to the oceans. *Nature Communications*, *5*(1), 3929. https://doi.org/10.1038/ncomms4929

Herraiz-Borreguero, L., Lannuzel, D., van der Merwe, P., Treverrow, A., & Pedro, J. B. (2016). Large flux of iron from the Amery Ice Shelf marine ice to Prydz Bay, East Antarctica. *Journal of Geophysical Research: Oceans*, *121*(8), 6009–6020. https://doi.org/10.1002/2016JC011687

Hersbach, H., Bell, B., Berrisford, P., Hirahara, S., Horányi, A., Muñoz-Sabater, J., et al. (2020). The ERA5 global reanalysis. *Quarterly Journal of the Royal Meteorological Society*, *146*(730), 1999–2049. https://doi.org/10.1002/qj.3803

Hosking, J. S., Orr, A., Marshall, G. J., Turner, J., & Phillips, T. (2013). The Influence of the Amundsen–Bellingshausen Seas Low on the Climate of West Antarctica and Its Representation in Coupled Climate Model Simulations. *Journal of Climate*, *26*(17), 6633–6648. https://doi.org/10.1175/JCLI-D-12-00813.1

Hosking, J. S., Orr, A., Bracegirdle, T. J., & Turner, J. (2016). Future circulation changes off West Antarctica: Sensitivity of the Amundsen Sea Low to projected anthropogenic forcing. *Geophysical Research Letters*, *43*(1), 367–376. https://doi.org/10.1002/2015GL067143

Jacobs, S. S., Jenkins, A., Giulivi, C. F., & Dutrieux, P. (2011). Stronger ocean circulation and increased melting under Pine Island Glacier ice shelf. *Nature Geoscience*, *4*(8), 519–523. https://doi.org/10.1038/ngeo1188

Jourdain, N. C., Mathiot, P., Merino, N., Durand, G., Le Sommer, J., Spence, P., et al. (2017). Ocean circulation and sea-ice thinning induced by melting ice shelves in the Amundsen Sea. *Journal of Geophysical Research: Oceans*, *122*(3), 2550–2573. https://doi.org/10.1002/2016JC012509

Kauko, H. M., Hattermann, T., Ryan-Keogh, T., Singh, A., de Steur, L., Fransson, A., et al. (2021). Phenology and Environmental Control of Phytoplankton Blooms in the Kong Håkon VII Hav in the Southern Ocean. *Frontiers in Marine Science*, *8*. https://doi.org/10.3389/fmars.2021.623856

https://doi.org/10.5194/egusphere-2025-3149
Preprint. Discussion started: 25 July 2025

Lannuzel, D., Fourquez, M., de Jong, J., Tison, J.-L., Delille, B., & Schoemann, V. (2023). First report on biological iron uptake in the Antarctic sea-ice environment. *Polar Biology*, *46*(4), 339–355. https://doi.org/10.1007/s00300-023-03127-7

Lee, S. H., Kim, B. K., Lim, Y. J., Joo, H., Kang, J. J., Lee, D., Park, J., Ha, S.-Y., and Lee, S. H.: Small phytoplankton contribution to the standing stocks and the total primary production in the Amundsen Sea, Biogeosciences, 14, 3705–3713, https://doi.org/10.5194/bg-14-3705-2017, 2017.

Liu, Y., Moore, J. C., Cheng, X., Gladstone, R. M., Bassis, J. N., Liu, H., et al. (2015). Ocean-driven thinning enhances iceberg calving and retreat of Antarctic ice shelves. *Proceedings of the National Academy of Sciences*, *112*(11), 3263–3268. https://doi.org/10.1073/pnas.1415137112

Marchese, C., Albouy, C., Tremblay, J.-É., Dumont, D., D'Ortenzio, F., Vissault, S., & Bélanger, S. (2017). Changes in phytoplankton bloom phenology over the North Water (NOW) polynya: a response to changing environmental conditions. *Polar Biology*, *40*(9), 1721–1737. https://doi.org/10.1007/s00300-017-2095-2

Meredith, M., M. Sommerkorn, S. Cassotta, C. Derksen, A. Ekaykin, A. Hollowed, G. Kofinas, A. Mackintosh, J. Melbourne-Thomas, M.M.C. Muelbert, G. Ottersen, H. Pritchard, and E.A.G. Schuur, 2019: Polar Regions. In: *IPCC Special Report on the Ocean and Cryosphere in a Changing Climate* [H.-O. Pörtner, D.C. Roberts, V. Masson-Delmotte, P. Zhai, M. Tignor, E. Poloczanska, K. Mintenbeck, A. Alegría, M. Nicolai, A. Okem, J. Petzold, B. Rama, N.M. Weyer (eds.)]. Cambridge University Press, Cambridge, UK and New York, NY, USA, pp. 203-320. https://doi.org/10.1017/9781009157964.005

Morales Maqueda, M. A. (2004). Polynya Dynamics: a Review of Observations and Modeling. *Reviews of Geophysics*, *42*(1), RG1004. https://doi.org/10.1029/2002RG000116

Moreau, S., Mostajir, B., Bélanger, S., Schloss, I. R., Vancoppenolle, M., Demers, S., & Ferreyra, G. A. (2015). Climate change enhances primary production in the western Antarctic Peninsula. *Global Change Biology*, *21*(6), 2191–2205. https://doi.org/10.1111/gcb.12878

Naughten, K. A., Meissner, K. J., Galton-Fenzi, B. K., England, M. H., Timmermann, R., & Hellmer, H. H. (2018). Future Projections of Antarctic Ice Shelf Melting Based on

https://doi.org/10.5194/egusphere-2025-3149
Preprint. Discussion started: 25 July 2025

CMIP5 Scenarios. *Journal of Climate*, *31*(13), 5243–5261. https://doi.org/10.1175/JCLI-D-17-0854.1

Naveira Garabato, A. C. N., Forryan, A., Dutrieux, P., Brannigan, L., Biddle, L. C., Heywood, K. J., et al. (2017). Vigorous lateral export of the meltwater outflow from beneath an Antarctic ice shelf. *Nature*, *542*(7640), 219–222. https://doi.org/10.1038/nature20825

Oh, J.-H., Noh, K. M., Lim, H.-G., Jin, E. K., Jun, S.-Y., & Kug, J.-S. (2022). Antarctic meltwater-induced dynamical changes in phytoplankton in the Southern Ocean. *Environmental Research Letters*, *17*(2), 024022. https://doi.org/10.1088/1748-9326/ac444e

Oliver, H., St-Laurent, P., Sherrell, R. M., & Yager, P. L. (2019). Modeling Iron and Light Controls on the Summer *Phaeocystis antarctica* Bloom in the Amundsen Sea Polynya. *Global Biogeochemical Cycles*, 2018GB006168. https://doi.org/10.1029/2018GB006168

Pan, J. B., Gierach, M. M., Stammerjohn, S., Schofiled, O., Meredith, M. P., Reynolds, R. A., vernet, M., Haumann, F. A., et al. (2025). Impact of glacial metlwater on phytoplnakton biomass along the Western Antarctic Peninsula. *Communication Earth & Environment, 6*(456). https://doi.org/10.1038/s43247-025-02435-6

Paolo, F. S., Fricker, H. A., & Padman, L. (2015). Volume loss from Antarctic ice shelves is accelerating. *Science*, *348*(6232), 327–331. https://doi.org/10.1126/science.aaa0940

Paolo, F. S., Fricker, H. A., & Padman, L. (2016). Constructing improved decadal records of Antarctic ice shelf height change from multiple satellite radar altimeters. *Remote Sensing of Environment*, *177*, 192–205. https://doi.org/10.1016/j.rse.2016.01.026

Paolo, F. S., Gardner, A. S., Greene, C. A., Nilsson, J., Schodlok, M. P., Schlegel, N.-J., & Fricker, H. A. (2023). Widespread slowdown in thinning rates of West Antarctic ice shelves. *The Cryosphere*, *17*(8), 3409–3433. https://doi.org/10.5194/tc-17-3409-2023

Park, J., Kim, J.-H., Kim, H., Hwang, J., Jo, Y.-H., & Lee, S. H. (2019). Environmental Forcings on the Remotely Sensed Phytoplankton Bloom Phenology in the Central Ross Sea Polynya. *Journal of Geophysical Research: Oceans*, *124*(8), 5400–5417. https://doi.org/10.1029/2019JC015222

Park, J., Kuzminov, F. I., Bailleul, B., Yang, E. J., Lee, S., Falkowski, P. G., & Gorbunov, M. Y. (2017). Light availability rather than Fe controls the magnitude of massive phytoplankton

https://doi.org/10.5194/egusphere-2025-3149
Preprint. Discussion started: 25 July 2025

bloom in the Amundsen Sea polynyas, Antarctica. *Limnology and Oceanography*, *62*(5), 2260–2276. https://doi.org/10.1002/lno.10565

Person, R., Aumont, O., Madec, G., Vancoppenolle, M., Bopp, L., & Merino, N. (2019). Sensitivity of ocean biogeochemistry to the iron supply from the Antarctic Ice Sheet explored with a biogeochemical model. *Biogeosciences*, *16*(18), 3583–3603. https://doi.org/10.5194/bg-16-3583-2019

Pritchard, H. D., Ligtenberg, S. R. M., Fricker, H. A., Vaughan, D. G., van den Broeke, M. R., & Padman, L. (2012). Antarctic ice-sheet loss driven by basal melting of ice shelves. *Nature*, *484*(7395), 502–505. https://doi.org/10.1038/nature10968

Racault, M.-F., Le Quéré, C., Buitenhuis, E., Sathyendranath, S., & Platt, T. (2012). Phytoplankton phenology in the global ocean. *Ecological Indicators*, *14*(1), 152–163. https://doi.org/10.1016/j.ecolind.2011.07.010

Randall-Goodwin, E., Meredith, M. P., Jenkins, A., Yager, P. L., Sherrell, R. M., Abrahamsen, E. P., et al. (2015). Freshwater distributions and water mass structure in the Amundsen Sea Polynya region, Antarctica. *Elementa: Science of the Anthropocene*, *3*, 000065. https://doi.org/10.12952/journal.elementa.000065

Rignot, E., Jacobs, S., Mouginot, J., & Scheuchl, B. (2013). Ice-Shelf Melting Around Antarctica. *Science*, *341*(6143), 266–270. https://doi.org/10.1126/science.1235798

Rignot, E., Mouginot, J., Scheuchl, B., van den Broeke, M., van Wessem, M. J., & Morlighem, M. (2019). Four decades of Antarctic Ice Sheet mass balance from 1979–2017. *Proceedings of the National Academy of Sciences*, *116*(4), 1095–1103. https://doi.org/10.1073/pnas.1812883116

Shepherd, A., Ivins, E., Rignot, E., Smith, B., van den Broeke, M., Velicogna, I., et al. (2018). Mass balance of the Antarctic Ice Sheet from 1992 to 2017. *Nature*, *558*(7709), 219–222. https://doi.org/10.1038/s41586-018-0179-y

Sherrell, R. M., Lagerström, M. E., Forsch, K. O., Stammerjohn, S. E., & Yager, P. L. (2015). Dynamics of dissolved iron and other bioactive trace metals (Mn, Ni, Cu, Zn) in the Amundsen Sea Polynya, Antarctica. *Elementa*, *3*, 000071. https://doi.org/10.12952/journal.elementa.000071

https://doi.org/10.5194/egusphere-2025-3149
Preprint. Discussion started: 25 July 2025

Siegel, D. A., Doney, S. C., & Yoder, J. A. (2002). The North Atlantic Spring Phytoplankton Bloom and Sverdrup's Critical Depth Hypothesis. *Science*, *296*(5568), 730–733. https://doi.org/10.1126/science.1069174

Smith, A. J. R., Nelson, T., Ratnarajah, L., Genovese, C., Westwood, K., Holmes, T. M., et al. (2022). Identifying potential sources of iron-binding ligands in coastal Antarctic environments and the wider Southern Ocean. *Frontiers in Marine Science*, *9*. https://doi.org/10.3389/fmars.2022.948772

Soppa, M. A., Völker, C., & Bracher, A. (2016). Diatom Phenology in the Southern Ocean: Mean Patterns, Trends and the Role of Climate Oscillations. *Remote Sensing*, *8*(5), 420. https://doi.org/10.3390/rs8050420

Stammerjohn, S. E., Martinson, D. G., Smith, R. C., & Iannuzzi, R. A. (2008). Sea ice in the western Antarctic Peninsula region: Spatio-temporal variability from ecological and climate change perspectives. *Deep Sea Research Part II: Topical Studies in Oceanography*, *55*(18–19), 2041–2058. https://doi.org/10.1016/j.dsr2.2008.04.026

St-Laurent, P., Yager, P. L., Sherrell, R. M., Stammerjohn, S. E., & Dinniman, M. S. (2017). Pathways and supply of dissolved iron in the Amundsen Sea (Antarctica). *Journal of Geophysical Research: Oceans*, *122*(9), 7135–7162. https://doi.org/10.1002/2017JC013162

St-Laurent, P., Yager, P. L., Sherrell, R. M., Oliver, H., Dinniman, M. S., & Stammerjohn, S. E. (2019). Modeling the Seasonal Cycle of Iron and Carbon Fluxes in the Amundsen Sea Polynya, Antarctica. *Journal of Geophysical Research: Oceans*, *124*(3), 1544–1565. https://doi.org/10.1029/2018JC014773

Tagliabue, A., Bowie, A. R., DeVries, T., Ellwood, M. J., Landing, W. M., Milne, A., et al. (2019). The interplay between regeneration and scavenging fluxes drives ocean iron cycling. *Nature Communications*, *10*(1), 4960. https://doi.org/10.1038/s41467-019-12775-5

Tamsitt, V., England, M. H., Rintoul, S. R., & Morrison, A. K. (2021). Residence Time and Transformation of Warm Circumpolar Deep Water on the Antarctic Continental Shelf. *Geophysical Research Letters*, *48*(20), e2021GL096092. https://doi.org/10.1029/2021GL096092

https://doi.org/10.5194/egusphere-2025-3149
Preprint. Discussion started: 25 July 2025

Tamura, T. P., Nomura, D., Hirano, D., Tamura, T., Kiuchi, M., Hashida, G., et al. (2022). Impacts of basal melting of the Totten Ice Shelf and biological productivity on marine biogeochemical components in Sabrina Coast, East Antarctica. *Global Biogeochemical Cycles*, *n/a*(n/a), e2022GB007510. https://doi.org/10.1029/2022GB007510

Thomalla, S. J., Ogunkoya, A. G., Vichi, M., & Swart, S. (2017). Using Optical Sensors on Gliders to Estimate Phytoplankton Carbon Concentrations and Chlorophyll-to-Carbon Ratios in the Southern Ocean. *Frontiers in Marine Science*, *4*. https://doi.org/10.3389/fmars.2017.00034

Thuróczy, C.-E., Alderkamp, A.-C., Laan, P., Gerringa, L. J. A., Mills, M. M., van Dijken, G. L., et al. (2012). Key role of organic complexation of iron in sustaining phytoplankton blooms in the Pine Island and Amundsen Polynyas (Southern Ocean). *Deep Sea Research Part II: Topical Studies in Oceanography*, *71–76*, 49–60. https://doi.org/10.1016/j.dsr2.2012.03.009

Turner, J., Hosking, J. S., Marshall, G. J., Phillips, T., & Bracegirdle, T. J. (2016). Antarctic sea ice increase consistent with intrinsic variability of the Amundsen Sea Low. *Climate Dynamics*, *46*(7–8), 2391–2402. https://doi.org/10.1007/s00382-015-2708-9

Vaillancourt, R. D., Sambrotto, R. N., Green, S., & Matsuda, A. (2003). Phytoplankton biomass and photosynthetic competency in the summertime Mertz Glacier Region of East Antarctica. *Deep Sea Research Part II: Topical Studies in Oceanography*, *50*(8–9), 1415–1440. https://doi.org/10.1016/S0967-0645(03)00077-8

van Manen, M., Aoki, S., Brussaard, C. P. D., Conway, T. M., Eich, C., Gerringa, L. J. A., et al. (2022). The role of the Dotson Ice Shelf and circumpolar deep water as driver and source of dissolved and particulate iron and manganese in the Amundsen Sea polynya, Southern Ocean. *Marine Chemistry*, 104161. https://doi.org/10.1016/j.marchem.2022.104161

Yager, P. L., Sherrell, R. M., Stammerjohn, S. E., Alderkamp, A.-C., Schofield, O., Abrahamsen, P., et al. (2012). ASPIRE: The Amundsen Sea Polynya International Research Expedition. *Oceanography*, *25*(3), 40–53. https://doi.org/10.5670/oceanog.2012.73

Yu, L.-S., He, H., Leng, H., Liu, H., & Lin, P. (2023). Interannual variation of summer sea surface temperature in the Amundsen Sea, Antarctica. *Frontiers in Marine Science*, *10*. https://doi.org/10.3389/fmars.2023.1050955

https://doi.org/10.5194/egusphere-2025-3149
Preprint. Discussion started: 25 July 2025

Zheng, Y., Heywood, K. J., Webber, B. G. M., Stevens, D. P., Biddle, L. C., Boehme, L., & Loose, B. (2021). Winter seal-based observations reveal glacial meltwater surfacing in the southeastern Amundsen Sea. *Communications Earth & Environment*, *2*(1), 1–9. https://doi.org/10.1038/s43247-021-00111-z